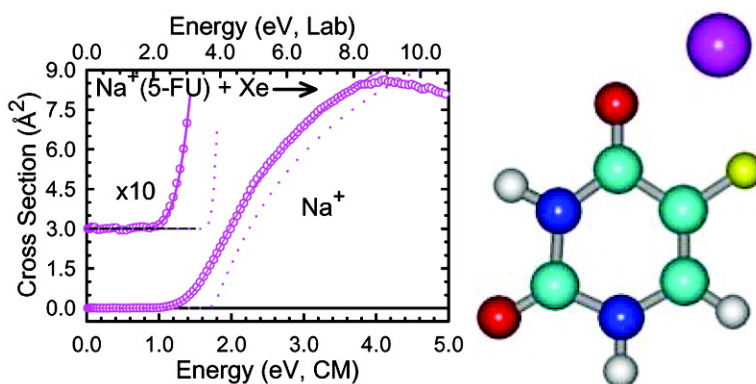


Influence of Halogenation on the Properties of Uracil and Its Noncovalent Interactions with Alkali Metal Ions. Threshold Collision-Induced Dissociation and Theoretical Studies

Zhibo Yang, and M. T. Rodgers

J. Am. Chem. Soc., **2004**, 126 (49), 16217-16226 • DOI: 10.1021/ja045375p • Publication Date (Web): 13 November 2004

Downloaded from <http://pubs.acs.org> on April 5, 2009



More About This Article

Additional resources and features associated with this article are available within the HTML version:

- Supporting Information
- Links to the 7 articles that cite this article, as of the time of this article download
- Access to high resolution figures
- Links to articles and content related to this article
- Copyright permission to reproduce figures and/or text from this article

[View the Full Text HTML](#)

Influence of Halogenation on the Properties of Uracil and Its Noncovalent Interactions with Alkali Metal Ions. Threshold Collision-Induced Dissociation and Theoretical Studies

Zhibo Yang and M. T. Rodgers*

Contribution from the Department of Chemistry, Wayne State University,
Detroit, Michigan 48202

Received July 31, 2004; E-mail: mroddgers@chem.wayne.edu

Abstract: The influence of halogenation on the properties of uracil and its noncovalent interactions with alkali metal ions is investigated both experimentally and theoretically. Bond dissociation energies of alkali metal ion-halouracil complexes, $M^+(XU)$, are determined using threshold collision-induced dissociation techniques in a guided ion beam mass spectrometer, where $M^+ = Li^+, Na^+, \text{ and } K^+$ and $XU = 5\text{-fluorouracil}, 5\text{-chlorouracil}, 6\text{-chlorouracil}, 5\text{-bromouracil}, \text{ and } 5\text{-iodouracil}$. The structures and theoretical bond dissociation energies of these complexes are determined from ab initio calculations. Theoretical calculations are also performed to examine the influence of halogenation on the acidities, proton affinities, and Watson-Crick base pairing energies. Halogenation of uracil is found to produce a decrease in the proton affinity, an increase in the alkali metal ion binding affinities, an increase in the acidity, and stabilization of the A::U base pair. In addition, alkali metal ion binding is expected to lead to an increase in the stability of nucleic acids by reducing the charge on the nucleic acid in a zwitterion effect as well as through additional noncovalent interactions between the alkali metal ion and the nucleobases.

Introduction

The 5-halouracils and their derivatives have demonstrated antitumor and antiviral properties.^{1–10} For example, 5-fluorouracil has been the most active agent employed in the chemotherapy of colorectal cancer.^{6,7} 5-Chlorouracil and 5-bromouracil have been studied to treat inflammatory tissue.^{8,9} Complexes of 5-iodouracil with a variety of transition metal ions (e.g., Mn^{2+} , Co^{2+} , Cu^{2+} , Zn^{2+} , and Cd^{2+}) have been shown to have antitumor activity.¹⁰ The 5- and 6-halouracils have also been investigated as a possible class of radio-sensitizers, which are used to control damage to healthy tissues in radiation therapy.¹¹ Although the mechanisms of the antitumor and antiviral action of these complexes is not well understood, it is likely that they inhibit the proper replication of DNA in tumor and infected cells. Thus, the properties and characteristics of the halouracils are of great interest in pharmaceutical research.

The participation of metal ions in biological processes is well-known. The presence of metal ions may influence the conformational behavior and function of DNA. For example, metal ions are crucial in determining which of numerous structures nucleic acids can assume, as well as the way that nucleic acids pack together.¹² Alkali metal ions, and other “hard” metal ions, have a low tendency to form covalent bonds and are therefore relatively nonspecific binders. Their primary influence is to neutralize the negative charges on the phosphate backbone, thereby stabilizing the double helix.^{13–16} Their interaction with the nucleobases also neutralizes the negative charges on the phosphate backbone in a zwitterion effect. In general, more profound effects on the stability and conformation of DNA are induced by metal ions that bind to the nucleobases than those that bind to the phosphate backbone.¹⁷ Thus, the interaction of metal ions with the nucleobases may provide supporting and fundamental information relevant to biology and pharmacology.

In recent work, we have developed methods to allow the application of quantitative threshold collision-induced dissociation (CID) methods to obtain accurate thermodynamic information on increasingly large systems.^{18–29} One of the driving forces

- (1) Jang, Y. H.; Sowers, L. C.; Cagin, T.; Goddard, W. A., III. *J. Phys. Chem. A* **2001**, *105*, 274.
- (2) Heidelberger, C. *Prog. Nucleic Acid Res. Mol. Biol.* **1965**, *4*, 1.
- (3) Rowe, W. P.; Lowy, D. R.; Teich, N.; Hartly, J. W. *Proc. Natl. Acad. Sci. U.S.A.* **1972**, *69*, 1033.
- (4) Sternglanz, H.; Bugg, C. E. *Biochim. Biophys. Acta* **1975**, *378*, 1.
- (5) Morris, S. M. *Mutat. Res.* **1993**, *297*, 39.
- (6) Takimoto, C. H.; Voeller, D. B.; Strong, J. M.; Anderson, L.; Chu, E.; Allegra, C. J. *J. Biol. Chem.* **1993**, *268*, 21438.
- (7) Germ, J. L. In *Cancer Chemotherapy: Principles & Practice*, 2nd ed.; Chabner, B. A., Collins, J. M., Eds.; J. B. Lippincott Co.: Philadelphia, PA, 1990; p 180.
- (8) Henderson, J. P.; Byun, J.; Takeshita, J.; Heinecke, J. W. *J. Biol. Chem.* **2003**, *278*, 23522.
- (9) Jiang, Q.; Blount, B. C.; Ames, B. N. *J. Biol. Chem.* **2003**, *278*, 32834.
- (10) Singh, U. P.; Singh, B. N.; Ghose, A. K.; Singh, R. K.; Sodhi, A. *J. Inorg. Biochem.* **1991**, *44*, 277.
- (11) Denifl, S.; Ptasińska, S.; Gstir, B.; Scheier, P.; Märk, T. D. *Int. J. Mass Spectrom.* **2004**, *232*, 99.

- (12) Eichhorn, G. L. *Adv. Inorg. Biochem.* **1981**, *3*, 1.
- (13) Shack, J.; Jenkins, R. J.; Thompsett, J. M. *J. Biol. Chem.* **1953**, *203*, 373.
- (14) Dove, W. F.; Davidson, N. *J. Mol. Biol.* **1962**, *5*, 467.
- (15) Eichhorn, G. L. *Nature* **1962**, *194*, 474.
- (16) Eichhorn, G. L.; Shin, Y. A. *J. Am. Chem. Soc.* **1968**, *90*, 7323.
- (17) Shin, Y. A.; Eichhorn, G. L. *Biopolymers* **1977**, *16*, 225.
- (18) Rodgers, M. T.; Armentrout, P. B. *J. Am. Chem. Soc.* **2000**, *122*, 8548.
- (19) Yang, Z.; Rodgers, M. T. *Int. J. Mass Spectrom.* Submitted.
- (20) Valina, A. B.; Amunugama, R.; Huang, H.; Rodgers, M. T. *J. Phys. Chem. A* **2001**, *105*, 11057.
- (21) Vitale, G.; Valina, A. B.; Huang, H.; Amunugama, R.; Rodgers, M. T. *J. Phys. Chem. A* **2001**, *105*, 11351.

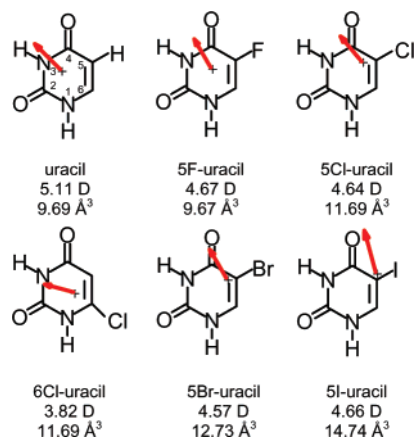


Figure 1. Structures of uracil (U) and the halouracils (XU). Properly scaled and oriented dipole moments in Debye are shown for each as an arrow. Dipole moments are determined from theoretical calculations performed here. The estimated polarizability is also shown.³⁰

behind these developments is our interest in applying such techniques to systems having biological relevance. In addition, we seek to perform accurate thermochemical measurements that provide absolute anchors for metal cation affinity scales over a broadening range of energies and classes of ligands. In the present paper, we examine the interactions of five halouracils: 5-fluorouracil (5-FU), 5-chlorouracil (5-CIU), 6-chlorouracil (6-ClU), 5-bromouracil (5-BrU), and 5-iodouracil (5-IU) with the alkali metal ions: Li⁺, Na⁺, and K⁺. The structures of the neutral XU nucleobases are shown in Figure 1 along with their calculated dipole moments and estimated polarizabilities.³⁰ Our study utilizes guided ion beam mass spectrometry to measure the cross sections for CID of 14 of these complexes. The Li⁺(5-IU) was not studied experimentally. The kinetic energy dependent CID cross sections are analyzed using methods developed previously that explicitly include the effects of the internal and translational energy distributions of the reactants, multiple collisions with Xe, and the lifetime for dissociation.²² We derive M⁺–XU bond dissociation energies (BDEs) for 14 M⁺(XU) complexes and compare these values to theoretical BDEs calculated here. Comparison is also made to literature values for the analogous complexes of the alkali metal ions with uracil (U).¹⁸ The trends in the measured and calculated BDEs are examined to determine the effects of halogenation on the properties of uracil and its noncovalent interactions with alkali metal ions. Theoretical calculations are also performed to examine the influence of halogenation on the acidities, proton affinities, and Watson–Crick base pairing energies, as well as implications for the stability of nucleic acids.

Experimental and Theoretical Section

Experimental Protocol. Cross sections for CID of M⁺(XU), where M⁺ = Li⁺, Na⁺, and K⁺ and XU = 5-FU, 5-CIU, 6-ClU, 5-BrU, and 5-IU, are measured using a guided ion beam mass spectrometer that

has been described in detail previously.³¹ The alkali metal ion–nucleobase complexes are formed by condensation of the alkali metal ion and neutral XU nucleobase in a flow tube ion source operating at pressures in the range from 0.5 to 0.7 Torr. The complexes are collisionally stabilized and thermalized to room temperature by in excess of 10⁵ collisions with the He and Ar bath gases, such that ions emanating from the source have an internal energy distribution that is well described by a Maxwell–Boltzmann distribution at 298 K. The ions are effusively sampled, focused, accelerated, and focused into a magnetic sector momentum analyzer for mass analysis. Mass-selected ions are decelerated to a desired kinetic energy and focused into an octopole ion guide. The octopole passes through a static gas cell containing Xe^{32–34} at sufficiently low pressures that multiple ion–neutral collisions are improbable, ~0.04–0.20 mTorr. The octopole ion guide acts as an efficient radial ion trap³⁵ such that scattered reactant and product ions are not lost as they drift toward the end of the octopole. These ions are focused into a quadrupole mass filter for mass analysis and subsequently detected with a secondary electron scintillation detector and standard pulse counting techniques.

In the present work, two different oscillators were used with the quadrupole mass filter, an 880 kHz and a 1.7 MHz oscillator with mass ranges that extend up to 1000 and 200 Da, respectively. The latter oscillator was purchased for use in experiments with very low mass product ions, e.g., Li⁺, to overcome low mass discrimination problems encountered with the 880 kHz oscillator. The use of this new resonator significantly improved collection of low mass ions. To ensure that the use of this new oscillator did not influence our thermochemical measurements, several systems were examined using both oscillators. The shapes (energy dependence) of the measured CID cross sections were preserved, and the threshold values determined using both resonators were consistent within experimental error for all systems tested. The magnitudes of the measured CID cross sections for the systems producing low mass product ions, i.e., Li⁺, were found to increase somewhat, whereas the systems with heavier product ions, i.e., Na⁺ and K⁺, were also preserved within the reported uncertainties.

Data Handling. Measured ion intensities are converted to absolute cross sections using a Beer's law analysis as described previously.³⁶ Errors in the pressure measurement and uncertainties in the length of the interaction region lead to ±20% uncertainties in the cross section magnitudes, while relative uncertainties are approximately ±5%.

Ion kinetic energies in the laboratory frame, E_{lab} , are converted to energies in the center-of-mass (CM) frame, E_{CM} . All energies reported below are in the CM frame unless otherwise noted. The absolute zero and distribution of the ion kinetic energies are determined using the octopole ion guide as a retarding potential analyzer, as previously described.³⁶ The distribution of ion kinetic energies is nearly Gaussian with a fwhm in the range from 0.2 to 0.5 eV (lab) for these experiments. The uncertainty in the absolute energy scale is ±0.05 eV (lab).

Because multiple ion–neutral collisions can influence the shape of CID cross sections and the threshold regions are most sensitive to these effects, the CID cross section for each complex was measured twice at three nominal pressures (0.05, 0.10, and 0.20 mTorr). Data free from pressure effects are obtained by extrapolating to zero reactant pressure, as described previously.^{32,37} Thus, results reported below are due to single bimolecular encounters.

Theoretical Calculations. To obtain model structures, vibrational frequencies, and energetics for the neutral, deprotonated, protonated,

- (22) Rodgers, M. T.; Ervin, K. M.; Armentrout, P. B. *J. Chem. Phys.* **1997**, *106*, 4499.
 (23) Huang, H.; Rodgers, M. T. *J. Phys. Chem. A* **2002**, *106*, 4277.
 (24) Chu, Y.; Yang, Z.; Rodgers, M. T. *J. Am. Soc. Mass Spectrom.* **2002**, *13*, 453.
 (25) Amunugama, R.; Rodgers, M. T. *J. Phys. Chem. A* **2002**, *106*, 5529.
 (26) Amunugama, R.; Rodgers, M. T. *J. Phys. Chem. A* **2002**, *106*, 9092.
 (27) Amunugama, R.; Rodgers, M. T. *J. Phys. Chem. A* **2002**, *106*, 9718.
 (28) Amunugama, R.; Rodgers, M. T. *Int. J. Mass Spectrom.* **2003**, *222*, 431.
 (29) Amunugama, R.; Rodgers, M. T. *Int. J. Mass Spectrom.* **2003**, *227*, 1.
 (30) Miller, K. J. *J. Am. Chem. Soc.* **1990**, *112*, 8533.

- (31) Rodgers, M. T. *J. Chem. Phys. A* **2001**, *11*, 2374.
 (32) Dalleska, N. F.; Honma, K.; Armentrout, P. B. *J. Am. Chem. Soc.* **1993**, *115*, 12125.
 (33) Aristov, N.; Armentrout, P. B. *J. Phys. Chem.* **1986**, *90*, 5135.
 (34) Hales, D. A.; Armentrout, P. B. *J. Cluster Sci.* **1990**, *1*, 127.
 (35) Teloy, E.; Gerlich, D. *Chem. Phys.* **1974**, *4*, 417. Gerlich, D. Diplomarbeit, University of Freiburg, Federal Republic of Germany, 1971. Gerlich, D. In *State-Selected and State-to-State Ion–Molecule Reaction Dynamics, Part I, Experiment*; Ng, C.-Y., Baer, M., Eds. *Adv. Chem. Phys.* **1992**, *82*, 1.
 (36) Ervin, K. M.; Armentrout, P. B. *J. Chem. Phys.* **1985**, *83*, 166.
 (37) Hales, D. A.; Lian, L.; Armentrout, P. B. *Int. J. Mass Spectrom. Ion Processes* **1990**, *102*, 269.

and alkali metalated nucleobases, theoretical calculations were performed using Gaussian 98.³⁸ For the systems excluding 5-IU, geometry optimizations and vibrational analyses were performed at the MP2(full)/6-31G* level. When used to model the data or to calculate thermal energy corrections, the MP2(full)/6-31G* vibrational frequencies are scaled by a factor of 0.9646.³⁹ The vibrational frequencies and rotational constants of the ground-state M⁺(XU) complexes and neutral XU nucleobases are listed in Tables 1S and 2S of the Supporting Information. Single-point energy calculations were performed at the MP2(full)/6-311+G(2d,2p) level using the MP2(full)/6-31G* geometries. Parameters for iodine are not available in the above basis sets; therefore, calculations for the 5-IU systems were performed using the LANL2DZ^{40,41} and modified LANL2DZ^{40,42} effective core potentials (ECPs) and valence basis sets for I, while the standard basis sets described above were used for all other atoms. To assess the accuracy of these calculations, the 5-BrU systems were also computed using the corresponding ECPs for Br. To obtain accurate BDEs, zero-point energy (ZPE) and basis set superposition error (BSSE) corrections were included in the determination of the BDEs.^{43,44}

We considered various possible binding sites to the nucleobases: O2 and O4. Stable minima were found for all three alkali metal ions at the O2 and O4 positions for all five XU nucleobases examined in this work. In previous work,¹⁸ complexes in which the alkali metal ion binds out of the plane of the molecule to the π electrons were found to be much less stable than the planar complexes (Table 2). Because halogen substituents are electron withdrawing, halogenation of uracil should slightly decrease the π electron density of the aromatic ring making the π complexes slightly less stable. Therefore, calculations for π binding conformations of the M⁺(XU) complexes were not pursued in the current study.

To examine the influence of halogenation on the stability of the A::U base pair, theoretical calculations were also performed. With the computational resources available, we were unable to perform these calculations at the same level of theory employed for the neutral and alkali metalated nucleobases. Therefore, geometry optimizations and vibrational analyses were performed at the B3LYP/6-31G* level of theory. ZPE corrections are computed using the vibrational frequencies scaled by a factor of 0.9804.³⁹ Single-point energy calculations and BSSE corrections^{43,44} were carried out at the MP2(full)/6-311+G(2d,2p) level using the B3LYP/6-31G* optimized geometries.

Thermochemical Analysis. The threshold regions of the reaction cross sections are modeled using eq 1

$$\sigma(E) = \sigma_0 \sum_i g_i (E + E_i - E_0)^n / E \quad (1)$$

- (38) Frisch, M. J.; Trucks, G. W.; Schlegel, H. B.; Scuseria, G. E.; Robb, M. A.; Cheeseman, J. R.; Zakrzewski, V. G.; Montgomery, J. A., Jr.; Stratmann, R. E.; Burant, J. C.; Dapprich, S.; Millam, J. M.; Daniels, A. D.; Kudin, K. N.; Strain, M. C.; Farkas, O.; Tomasi, J.; Barone, V.; Cossi, M.; Cammi, R.; Mennucci, B.; Pomelli, C.; Adamo, C.; Clifford, S.; Ochterski, J.; Petersson, G. A.; Ayala, P. Y.; Cui, Q.; Morokuma, K.; Malick, D. K.; Rabuck, A. D.; Raghavachari, K.; Foresman, J. B.; Cioslowski, J.; Ortiz, J. V.; Baboul, A. G.; Stefanov, B. B.; Liu, G.; Liashenko, A.; Piskorz, P.; Komaromi, I.; Gomperts, R.; Martin, R. L.; Fox, D. J.; Keith, T.; Al-Laham, M. A.; Peng, C. Y.; Nanayakkara, A.; Gonzalez, C.; Challacombe, M.; Gill, P. M. W.; Johnson, B.; Chen, W.; Wong, M. W.; Andres, J. L.; Gonzalez, C.; Head-Gordon, M.; Replogle, E. S.; Pople, J. A. *Gaussian 98*, revision A.11; Gaussian, Inc.: Pittsburgh, PA, 1998.
- (39) *Exploring Chemistry with Electronic Structures Methods*, 2nd ed.; Foresman, J. B.; Frisch, A. E. Gaussian: Pittsburgh, PA, 1996.
- (40) Basis sets were obtained from the Extensible Computational Chemistry Environment Basis Set Database, Version 10/21/03, as developed and distributed by the Molecular Science Computing Facility, Environmental and Molecular Sciences Laboratory, which is part of the Pacific Northwest Laboratory, P.O. Box 999, Richland, WA 99352, USA, and funded by the U.S. Department of Energy. The Pacific Northwest Laboratory is a multiprogram laboratory operated by Battelle Memorial Institute for the U.S. Department of Energy under Contract DE-AC06-76RLO 1830. Contact David Feller or Karen Schuchardt for further information.
- (41) Hay, P. J.; Wadt, W. R. *J. Chem. Phys.* **1985**, *82*, 299.
- (42) Check, C. E.; Faust, T. O.; Bailey, J. M.; Wright, B. J.; Gilbert, T. M.; Sunderlin, L. S. *J. Phys. Chem. A* **2001**, *105*, 8111.

where σ_0 is an energy independent scaling factor, E is the relative translational energy of the reactants, E_0 is the threshold for reaction of the ground electronic and ro-vibrational state, and n is an adjustable parameter that describes the efficiency of kinetic to internal energy transfer.⁴⁵ The summation is over the ro-vibrational states of the reactant ions, i , where E_i is the excitation energy of each state and g_i is the population of those states ($\sum g_i = 1$).

The Beyer–Swinehart algorithm⁴⁶ is used to evaluate the density of the ro-vibrational states, i , and the relative populations of those states, g_i , are calculated by a Maxwell–Boltzmann distribution at 298 K, the temperature appropriate for the reactants. Vibrational frequencies and rotational constants of the reactant complexes are determined from theoretical calculations as described in the Theoretical Calculations section. The average vibrational energies at 298 K of the M⁺(XU) complexes are given in the Supporting Information, Table 1S. Inaccuracies in the computed frequencies are accounted for by increasing and decreasing the prescaled frequencies by 10% as suggested by Pople et al.⁴⁷ The corresponding change in the average vibrational energy is taken to be an estimate of one standard deviation of the uncertainty in the vibrational energy (Table 1S).

We also consider the possibility that collisionally activated complex ions do not dissociate on the time scale of our experiment ($\sim 10^{-4}$ s) by including statistical theories for unimolecular dissociation into eq 1 as described in detail elsewhere.^{22,48} This requires sets of ro-vibrational frequencies appropriate for the energized molecules and the transition states (TSs) leading to dissociation. The former are given in Tables 1S and 2S, while we assume that the TSs are loose and productlike because the interaction between the alkali metal ion and the nucleobase is largely electrostatic, a treatment that corresponds to a phase space limit (PSL), as described in detail elsewhere.²² In the present work, the adiabatic 2-D rotational energy is treated using a statistical distribution with explicit summation over the possible values of the rotational quantum number.²²

The model represented by eq 1 is expected to be appropriate for translationally driven reactions⁴⁹ and has been found to reproduce reaction cross sections well in numerous previous studies of CID processes. The model is convoluted with the kinetic energy distributions of the reactants, and a nonlinear least-squares analysis of the data is performed to give optimized values for the parameters σ_0 , E_0 , and n . The error associated with the measurement of E_0 is estimated from the range of threshold values determined for the eight zero-pressure-extrapolated data sets for each complex, variations associated with uncertainties in the vibrational frequencies (scaling as discussed above), and the error in the absolute energy scale, 0.05 eV (lab). For analyses that include the RRKM lifetime analysis, the uncertainties in the reported E_0 (PSL) values also include the effects of increasing and decreasing the time assumed available for dissociation by a factor of 2.

Equation 1 explicitly includes the internal energy of the ion, E_i . All energy available is treated statistically because the internal energy of the reactants is redistributed throughout the ion upon collision with Xe. Because the CID processes examined here are simple noncovalent bond fission reactions, the E_0 (PSL) values determined by analysis with eq 1 can be equated to 0 K BDEs.^{50,51}

- (43) Boys, S. F.; Bernardi, R. *Mol. Phys.* **1979**, *19*, 553.
- (44) Van Duijneveldt, F. B.; van Duijneveldt-van de Rijdt, J. G. C. M.; van Lenthe, J. H. *Chem. Rev.* **1994**, *94*, 1873.
- (45) Muntean, F.; Armentrout, P. B. *J. Chem. Phys.* **2001**, *115*, 1213.
- (46) Beyer, T. S.; Swinehart, D. F. *Commun. ACM* **1973**, *16*, 379. Stein, S. E.; Rabinovitch, B. S. *J. Chem. Phys.* **1973**, *58*, 2438; *Chem. Phys. Lett.* **1977**, *49*, 1883.
- (47) Pople, J. A.; Schlegel, H. B.; Raghavachari, K.; DeFrees, D. J.; Binkley, J. F.; Frisch, M. J.; Whitesides, R. F.; Hout, R. F.; Hehre, W. J. *Int. J. Quantum Chem. Symp.* **1981**, *15*, 269. DeFrees, D. J.; McLean, A. D. *J. Chem. Phys.* **1985**, *82*, 333.
- (48) Khan, F. A.; Clemmer, D. E.; Schultz, R. H.; Armentrout, P. B. *J. Phys. Chem.* **1993**, *97*, 7978.
- (49) Chesnavich, W. J.; Bowers, M. T. *J. Phys. Chem.* **1979**, *83*, 900.

Table 1. Fitting Parameters of Equation 1, Threshold Dissociation Energies at 0 K, and Entropies of Activation at 1000 K^a

reactant complex	σ_0^b	n^b	E_0^c (eV)	$E_0(\text{PSL})$ (eV)	kinetic shift (eV)	$\Delta S^\ddagger(\text{PSL})$ (J mol ⁻¹ K ⁻¹)
Li ⁺ (5-FU)	0.3 (0.02)	1.8 (0.1)	2.33 (0.05)	2.06 (0.05)	0.27	41 (2)
Na ⁺ (5-FU)	15.0 (0.6)	1.0 (0.03)	1.69 (0.05)	1.54 (0.04)	0.15	34 (2)
K ⁺ (5-FU)	10.2 (0.2)	1.3 (0.1)	1.21 (0.04)	1.14 (0.04)	0.07	29 (2)
Li ⁺ (5-CIU)	0.8 (0.1)	1.2 (0.1)	3.01 (0.10)	2.52 (0.09)	0.49	37 (2)
Na ⁺ (5-CIU)	3.4 (0.2)	1.2 (0.07)	1.58 (0.04)	1.47 (0.04)	0.09	34 (2)
K ⁺ (5-CIU)	25.5 (1.3)	1.3 (0.06)	1.10 (0.04)	1.08 (0.03)	0.02	25 (2)
Li ⁺ (6-CIU)	0.7 (0.1)	1.3 (0.1)	2.89 (0.09)	2.38 (0.08)	0.51	27 (2)
Na ⁺ (6-CIU)	2.8 (0.02)	1.2 (0.1)	1.65 (0.05)	1.45 (0.05)	0.20	24 (2)
K ⁺ (6-CIU)	6.1 (0.1)	1.4 (0.02)	1.05 (0.03)	1.01 (0.02)	0.04	21 (2)
Li ⁺ (5-BrU)	0.7 (0.1)	1.6 (0.1)	2.93 (0.07)	2.44 (0.05)	0.49	35 (2)
Na ⁺ (5-BrU)	9.5 (0.8)	1.4 (0.2)	1.60 (0.06)	1.48 (0.05)	0.12	35 (2)
K ⁺ (5-BrU)	25.3 (0.4)	1.2 (0.03)	1.23 (0.03)	1.14 (0.02)	0.09	30 (2)
Na ⁺ (5-IU)	2.8 (0.3)	1.4 (0.1)	1.69 (0.07)	1.53 (0.06)	0.16	33 (2)
K ⁺ (5-IU)	8.8 (2.9)	1.2 (0.2)	1.30 (0.06)	1.22 (0.05)	0.08	26 (2)

^a Uncertainties are listed in parentheses. ^b Average values for loose PSL transition state. ^c No RRKM analysis.

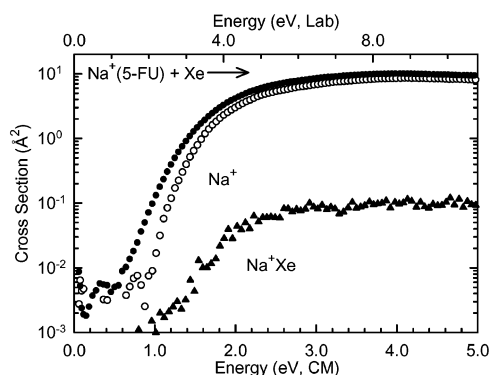
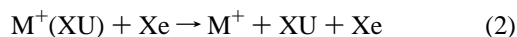


Figure 2. Cross sections for the collision-induced dissociation of the Na⁺(5-FU) complex with Xe as a function of kinetic energy in the center-of-mass frame (lower x-axis) and laboratory frame (upper x-axis). Data for Na⁺ product channel are shown for a Xe pressure of 0.2 mTorr (●) and extrapolated to zero (○). The cross section for the ligand exchange process to form Na⁺Xe is also shown (▲).

Results

Cross Sections for Collision-Induced Dissociation. Experimental cross sections were obtained for the interaction of Xe with 14 M⁺(XU) complexes, where M⁺ = Li⁺, Na⁺, and K⁺ and XU = 5-FU, 5-CIU, 6-CIU, 5-BrU, and 5-IU. The Li⁺(5-IU) was not studied experimentally due to low mass discrimination of our 880 kHz resonator (with a mass range that extends up to 1000 Da) and the upper mass limit of our 1.7 MHz resonator (with a mass range that is limited to 200 Da). Figure 2 shows representative data for the Na⁺(5-FU) complex. Results for all other complexes are similar and are shown in Figure 1S in the Supporting Information. The dominant process for all complexes is the loss of the intact neutral XU nucleobase in the CID reactions 2.



The magnitudes of the cross sections increase from Li⁺ to Na⁺ to K⁺. This is largely because the thresholds decrease in that same order. In several systems, ligand exchange processes to form M⁺Xe are also observed as minor reaction pathways, reactions 3.



The cross sections for these products are more than 2 orders of

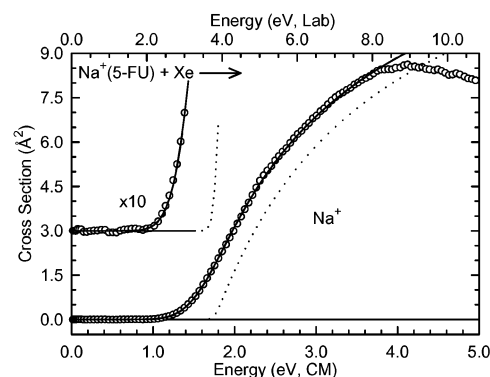


Figure 3. Zero pressure extrapolated cross section for collision-induced dissociation of the Na⁺(5-FU) complex with Xe in the threshold region as a function of kinetic energy in the center-of-mass frame (lower x-axis) and laboratory frame (upper x-axis). The solid line shows the best fit to the data using eq 1 convoluted over the neutral and ion kinetic and internal energy distributions. A dashed line shows the model cross sections in the absence of experimental kinetic energy broadening for reactants with an internal energy corresponding to 0 K.

magnitude smaller than those for the primary M⁺ product. It is likely that this ligand exchange process occurs for all complexes, but that the signal-to-noise in the other experiments was not sufficient to differentiate the M⁺Xe product from background noise. As little systematic information can be gleaned from these products, they will not be discussed further.

Threshold Analysis. The model of eq 1 was used to analyze the thresholds for reactions 2 in 14 M⁺(XU) systems. The results of these analyses are provided in Table 1, and representative results are shown in Figure 3 for the Na⁺(5-FU) complex. Results for all other complexes are shown in Figure 2S of the Supporting Information. In all cases, the experimental cross sections for reactions 2 are accurately reproduced using a loose PSL TS model.²² Previous work has shown that this model provides the most accurate assessment of the kinetic shifts for CID processes for electrostatic ion–molecule complexes.^{18–22} Good reproduction of the data is obtained over energy ranges exceeding 2 eV and cross section magnitudes of at least a factor of 100. Table 1 also includes values of E_0 obtained without including the RRKM lifetime analysis. Comparison of these values with the $E_0(\text{PSL})$ values shows that the kinetic shifts

(50) Armentrout, P. B. In *Advances in Gas-Phase Ion Chemistry*; Adams, N. G., Babcock, L. M., Eds.; JAI: Greenwich, 1992; Vol. 1, pp 83–119.

(51) Armentrout, P. B.; Simons, J. *J. Am. Chem. Soc.* **1992**, *114*, 8627.

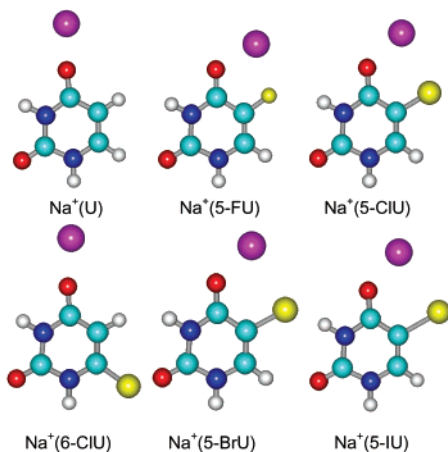


Figure 4. MP2(full)/6-31G* optimized geometries of $\text{Na}^+(\text{XU})$, where X = H, 5-F, 5-Cl, 6-Cl, 5-Br, and 5-I.

are largest for the most strongly bound systems, such that the kinetic shifts for the K^+ complexes are ≤ 0.09 eV, increase for the Na^+ complexes, 0.09 to 0.20 eV, and are even larger for the Li^+ complexes, 0.27 to 0.51 eV. This is the expected trend because the kinetic shift should correlate with the density of states of the activated complex at the threshold, which increases with energy.

The entropy of activation, ΔS^\ddagger , is a measure of the looseness of the TS and also a reflection of the complexity of the system. It is determined by the molecular parameters used to model the energized molecule and the TS, but also depends on the threshold energy. Listed in Table 1, $\Delta S^\ddagger(\text{PSL})$ values at 1000 K show modest variation and vary between 21 and 41 J/K mol across these systems. The values are largest for the Li^+ complexes and decrease with increasing size of the alkali metal cation. The $\Delta S^\ddagger(\text{PSL})$ values for $\text{M}^+(5\text{-XU})$ complexes are larger than those for the corresponding $\text{M}^+(6\text{-ClU})$ systems. The chelation interaction of the halo-substituent with the alkali metal ion in the $\text{M}^+(5\text{-XU})$ complexes constrains the motion of the halo-substituent, leading to a larger entropy change upon dissociation, because this motion is no longer constrained. These entropies of activation are similar to those determined for a wide variety of noncovalently bound complexes previously measured in our laboratory.

Theoretical Results. Theoretical structures for the neutral, deprotonated, protonated, and alkali metalated XU nucleobases, as well as the Watson–Crick base pairs between the XU nucleobases and adenine, were calculated as described in the Theoretical Calculations section. Details of the optimized geometries for the ground state conformations are provided in the Supporting Information, Table 3S. Results for the most stable conformations of the $\text{Na}^+(\text{XU})$ complexes are shown in Figure 4.⁵² Structures for the $\text{Li}^+(\text{XU})$ and $\text{K}^+(\text{XU})$ complexes are very similar to those for $\text{Na}^+(\text{XU})$ except for the $\text{M}^+\text{-XU}$ bond distance. The 0 K calculated proton and alkali metal ion binding energies are listed in Tables 2 and 3. Independent ZPE and BSSE corrections are made for all conformers listed. Geometrical parameters of the ground-state geometry optimized structures of the neutral, protonated, and alkali metalated XU nucleobases are listed in Table 4. The 0 K calculated acidities

Table 2. Calculated Enthalpies of Proton and Alkali Metal Ion Binding to Halouracils at 0 K in kJ/mol

complex	experiment		binding site	theory			
	TCID ^a	literature		D_0^c	MP2(full) ^b		
					D_0^d	$D_{0,\text{BSSE}}^e$	
$\text{H}^+(\text{U})^f$		866.6 ^g	O4	879.5	846.7	837.5	
		868 (13) ^h	O2	867.6	835.5	826.4	
		835 (13) ^h	O2	845.2	815.1	805.8	
$\text{Li}^+(\text{U})^f$	211.5 (6.1)		O4	840.2	810.4	801.0	
			O2	192.0	186.7	180.5	
			p	68.3	65.0	56.5	
$\text{Na}^+(\text{U})^f$	134.6 (3.4)		O4	146.2	142.5	134.5	
			O2	132.6	129.7	122.8	
			O4	110.8	107.8	103.8	
$\text{K}^+(\text{U})^f$	104.3 (2.8)		O2	98.4	96.1	92.2	
			O4	857.5	825.2	815.8	
			O2	836.2	804.5	795.5	
$\text{H}^+(5\text{-FU})$			O2	830.5	800.2	790.9	
			O4	826.3	796.3	786.9	
			O2	204.5	198.1	189.5	
$\text{Li}^+(5\text{-FU})$	198.9 (4.8)		O4	182.5	177.1	170.8	
			O2	145.6	142.1	133.9	
			O2	124.2	121.2	114.4	
$\text{Na}^+(5\text{-FU})$	149.0 (4.3)		O4	110.0	107.5	102.8	
			O2	90.7	88.4	84.5	
			O4	868.2	835.8	825.7	
$\text{K}^+(5\text{-FU})$	110.2 (3.8)		O4	845.1	813.6	804.0	
			O2	833.7	803.9	794.6	
			O2	829.4	799.8	790.5	
$\text{H}^+(5\text{-ClU})$			O4	213.1	206.4	197.4	
			O2	183.6	178.5	172.3	
			O4	149.4	145.7	136.9	
$\text{Li}^+(5\text{-ClU})$	242.9 (8.2)		O2	125.1	122.4	115.5	
			O4	113.5	110.7	105.7	
			O2	91.5	89.4	85.5	
$\text{Na}^+(5\text{-ClU})$	141.4 (3.4)		O4	871.5	839.1	829.8	
			O2	859.4	827.7	818.5	
			O2	830.4	800.4	791.1	
$\text{K}^+(5\text{-ClU})$	104.1 (2.7)		O4	825.6	795.8	786.5	
			O2	200.5	194.5	188.0	
			O4	182.1	177.0	170.5	
$\text{H}^+(6\text{ClU})$			O4	139.9	136.4	129.3	
			O2	124.6	121.7	114.6	
			O4	105.0	102.8	98.7	
$\text{Li}^+(6\text{ClU})$	229.6 (7.8)		O2	91.2	89.1	84.9	
			O4	872.6	840.1	829.5	
			O2	848.5	816.9	807.2	
$\text{Na}^+(6\text{ClU})$	139.5 (4.4)		O2	835.5	805.7	796.4	
			O4	831.1	801.7	792.3	
			O4	216.0	209.2	199.5	
$\text{K}^+(6\text{ClU})$	97.8 (2.2)		O4	184.4	179.4	173.1	
			O2	151.0	147.2	138.0	
			O2	125.7	123.1	116.2	
$\text{H}^+(5\text{-BrU})$			O4	114.1	111.3	106.0	
			O2	92.2	90.0	86.0	
			O4	235.9 (5.3)			
O2	184.4	179.4	173.1				
O2	151.0	147.2	138.0				
$\text{Li}^+(5\text{-BrU})$	235.9 (5.3)		O4	125.7	123.1	116.2	
			O2	114.1	111.3	106.0	
			O2	92.2	90.0	86.0	
$\text{Na}^+(5\text{-BrU})$	142.3 (4.8)		O4	109.8 (2.3)			
			O2				
			O2				
$\text{K}^+(5\text{-BrU})$	109.8 (2.3)		O4				
			O2				
			O2				

^a Present results, threshold collision-induced dissociation except as noted.

^b Calculated at the MP2(full)/6-311+G(2d,2p) level of theory using MP2(full)/6-31G* optimized geometries. ^c Calculated equilibrium BDEs.

^d Also includes ZPE corrections with frequencies scaled by 0.9646. ^e Also includes BSSE corrections. ^f Reference 18. ^g Reference 57. ^h Reference 58.

of the XU nucleobases are listed in Table 5. The 0 K calculated base pairing energies of the A::XU Watson–Crick base pairs are listed in Table 6, while the optimized structures of these base pairs are shown in Figure 5.

Dipole Moments. The calculated dipole moments of U and the XU nucleobases are summarized in Figure 1. Because the halogens have much larger masses and are more electronegative than hydrogen, the center-of-mass and electron density distribution of uracil are altered upon halo-substitution. In all cases, the center of the dipole moment moves toward the halo-

(52) Figures were generated using the output of Gaussian98 geometry optimizations in Hyperchem Computational Chemistry Software Package, version 5.0, Hypercube Inc., 1997.

Table 3. Calculated Enthalpies of Proton and Alkali Metal Ion Binding to Halouracils at 0 K in kJ/mol

complex	TCID ^a	experiment binding site	theory					
			LANL2DZ ^{b,c}			modified LANL2DZ ^{b,d}		
			D _e ^e	D ₀ ^f	D _{0,BSSE} ^g	D _e ^e	D ₀ ^f	D _{0,BSSE} ^g
H ⁺ (5-BrU)		O4	875.0	842.6	831.4	873.1	840.7	829.9
		O2	854.6	823.0	812.4	850.1	818.6	808.5
			841.4	811.8	802.4	837.0	807.3	798.0
			837.1	807.8	798.3	832.6	803.3	793.9
Li ⁺ (5-BrU)	235.9 (5.3)	O4	219.2	212.2	195.4	217.5	210.8	199.2
		O2	188.7	183.8	177.3	185.4	180.5	174.1
Na ⁺ (5-BrU)	142.3 (4.8)	O4	150.5	146.6	134.1	151.4	147.7	137.6
		O2	129.6	127.0	120.0	126.6	124.0	117.1
K ⁺ (5-BrU)	109.8 (2.3)	O4	113.4	110.6	104.7	114.4	111.7	106.2
		O2	95.4	93.5	89.3	92.8	90.9	86.8
H ⁺ (5-IU)		O4	881.8	849.5	837.8	878.6	846.4	835.5
		O2	862.3	830.7	819.3	856.1	824.6	814.5
			847.0	817.5	808.1	841.4	811.9	802.4
			842.7	813.5	804.0	837.0	807.8	798.3
Li ⁺ (5-IU)		O4	228.0	221.0	200.3	220.7	214.1	203.1
		O2	191.8	187.0	180.4	187.7	182.9	176.5
Na ⁺ (5-IU)	139.5 (4.4)	O4	155.3	151.5	137.0	153.4	149.7	140.1
		O2	132.1	129.6	122.4	128.5	126.0	119.0
K ⁺ (5-IU)	97.8 (2.2)	O4	115.5	112.7	106.6	115.8	113.1	107.8
		O2	97.6	95.8	91.6	94.4	92.6	88.6

^a Present results, threshold collision-induced dissociation. ^b Calculated at the MP2(full)/6-311+G(2d,2p) level of theory using MP2(full)/6-31G* optimized geometries. ^c Calculated by using LANL2DZ ECP for Br and I atoms. ^d Calculated using modified LANL2DZ for Br and I atoms. ^e Calculated equilibrium BDEs. ^f Also includes ZPE corrections with frequencies scaled by 0.9646. ^g Also includes BSSE corrections.

Table 4. Geometrical Parameters of MP2(full)/6-31G* Geometry Optimized Structures of Neutral, Protonated, and Alkali Metalated Halouracils

species	bond distance (Å)					bond angle (deg)	
	C=O	M ⁺ -O	C-X	M ⁺ -X	N3-H	∠COM ⁺	∠CXM ⁺
U	1.226				1.017		
H ⁺ (U)	1.315	0.980			1.024	112.4	
Li ⁺ (U)	1.263	1.750			1.019	171.9	
Na ⁺ (U)	1.255	2.109			1.019	173.2	
K ⁺ (U)	1.249	2.482			1.018	174.7	
5-FU	1.223		1.344		1.017		
H ⁺ (5-FU)	1.309	0.984	1.340		1.025	111.1	
Li ⁺ (5-FU)	1.254	1.878	1.377	2.052	1.022	112.1	106.4
Na ⁺ (5-FU)	1.247	2.230	1.370	2.424	1.021	118.2	111.3
K ⁺ (5-FU)	1.242	2.587	1.364	2.826	1.020	124.3	115.5
5-CIU	1.223		1.717		1.017		
H ⁺ (5-CIU)	1.309	0.984	1.712		1.024	111.5	
Li ⁺ (5-CIU)	1.254	1.840	1.729	2.553	1.021	123.6	90.7
Na ⁺ (5-CIU)	1.247	2.190	1.728	2.921	1.020	130.4	95.4
K ⁺ (5-CIU)	1.242	2.540	1.724	3.513	1.019	142.3	97.1
6-CIU	1.226		1.720		1.017		
H ⁺ (6-CIU)	1.316	0.980	1.690		1.023	112.4	
Li ⁺ (6-CIU)	1.263	1.751	1.702		1.019	172.2	
Na ⁺ (6-CIU)	1.254	2.114	1.705		1.018	172.4	
K ⁺ (6-CIU)	1.249	2.489	1.708		1.018	173.9	
5-BrU	1.223		1.875		1.018		
H ⁺ (5-BrU)	1.308	0.986	1.873		1.024	110.8	
Li ⁺ (5-BrU)	1.254	1.843	1.889	2.605	1.021	124.5	87.0
Na ⁺ (5-BrU)	1.246	2.199	1.887	2.959	1.020	131.0	91.8
K ⁺ (5-BrU)	1.241	2.552	1.884	3.390	1.020	139.3	95.6
5-IU	1.202		1.950		1.020		
H ⁺ (5-IU)	1.310	0.980	2.080		1.020	111.1	
Li ⁺ (5-IU)	1.250	1.830	2.080	2.800	1.020	130.4	81.2
Na ⁺ (5-IU)	1.248	2.181	2.080	3.230	1.020	137.4	85.6
K ⁺ (5-IU)	1.244	2.530	2.080	3.830	1.019	150.0	87.4

^a Reference 18.

substituent. The orientation and electron withdrawing character of the halo-substituent result in a modest decrease (~10%) in

Table 5. Calculated Enthalpies of Deprotonation of Uracil and Halouracils at 0 K in kJ/mol

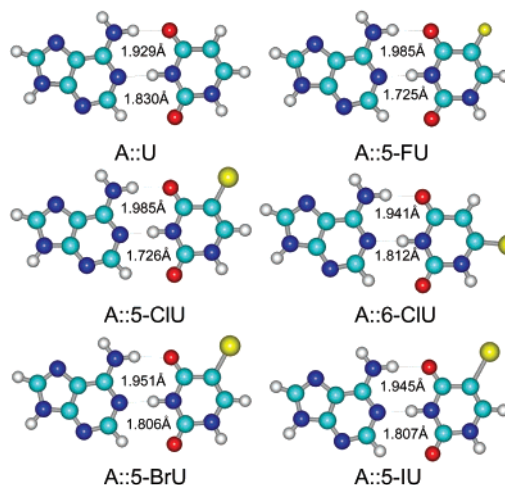
species	deprotonation site	theory (MP2(full)) ^a			literature	
		D _e ^b	D ₀ ^c	D _{0,BSSE} ^d	experiment	theory
U	N1	1422.5	1387.0	1377.0	1393 (17) ^e	1390.7 ^f 1391 ^g 1377 ^h
5-FU	N1	1402.2	1368.3	1358.3		
5-CIU	N1	1393.4	1359.8	1349.5		
6-CIU	N1	1377.2	1343.5	1333.1		
5-BrU	N1	1390.7	1357.0	1346.7		
5-IU	N1	1390.9	1357.3	1347.0		
U	N3	1475.3	1436.5	1426.4	1452 (17) ^e	1440.2 ^f 1447 ^g 1433 ^h
5-FU	N3	1447.2	1410.0	1399.8		
5-CIU	N3	1444.1	1408.1	1397.7		
6-CIU	N3	1447.0	1409.3	1399.2		
5-BrU	N3	1442.0	1405.2	1394.8		
5-IU	N3	1443.0	1406.2	1395.8		

^a MP2(full)/6-311+G(2d,2p)//MP2(full)/6-31G*. ^b Calculated equilibrium bond dissociation energies. ^c Also includes ZPE corrections. ^d Also includes BSSE corrections. ^e Reference 53. ^f Reference 19, CBS-Q. ^g Reference 54, B3LYP/6-31++G**. ^h Reference 55, B3LYP/6-31+G*.

Table 6. Calculated Hydrogen Bond Lengths and Enthalpies of Base Pairing of A::U and A::(XU) at 0 K^a

base pair	hydrogen bond lengths (Å)		enthalpies of base pairing (kJ/mol)		
	NH...N	NH...O	D _e ^b	D ₀ ^c	D _{0,BSSE} ^d
A::U	1.830	1.929	69.9	63.9	51.0
A::(5-FU)	1.725	1.985	72.3	66.4	52.6
A::(5-CIU)	1.726	1.985	73.2	67.5	53.7
A::(6-CIU)	1.812	1.941	72.5	66.8	53.4
A::(5-BrU)	1.806	1.951	73.8	67.7	53.3
A::(5-IU)	1.807	1.945	73.9	67.7	52.5

^a MP2(full)/6-311+G(2d,2p)//B3LYP/6-31G*. ^b Calculated equilibrium BDEs. ^c Also includes ZPE corrections. ^d Also includes BSSE corrections.

**Figure 5.** MP2(full)/6-31G* optimized geometries of A::XU base pairs, where X = H, 5-F, 5-CI, 6-Cl, 5-Br, and 5-I.

the magnitude of the dipole moment for the 5-XU nucleobases and a much larger decrease (~25%) for 6-CIU.

Alkali Metal Ion Binding. The optimized structures obtained for the isolated XU and M⁺(XU) are summarized in Tables 4 and 3S. In all cases, the nucleobases and their alkali metal ion complexes are planar. Similar to that found for uracil, the calculations find that the preferred binding site for all three alkali metal ions to all of the halouracils is at the O4 position.¹⁸ The

C=O—M⁺ bond angle is very nearly linear but shifted slightly toward the chloride atom in the complexes of 6-ClU. It is interesting to note that this shift is *away* from the global dipole moment of 6-ClU. In the 5-XU systems, the alkali metal ion chelates with O4 and the halogen atom such that the C=O—M⁺ bond angles decrease and vary from 112° to 150°. The C=O—M⁺ angles increase with the size of the alkali metal ion for a given nucleobase and with the size of the halogen substituent for a given alkali metal ion.

In previous work on uracil, the O2 binding site was found to be less favorable than O4 by 14.4, 11.7, and 11.6 kJ/mol for Li⁺, Na⁺, and K⁺, respectively.¹⁸ Halogenation at the 5- or 6-positions leads to a small increase in the differences in the relative O2 and O4 alkali metal ion binding affinities, 17.5 to 26.6 kJ/mol for Li⁺, 14.7 to 21.4 kJ/mol for Na⁺, and 13.8 to 20.2 kJ/mol for K⁺. The possibility that the metal ion might bind to the π electrons above the uracil ring was also investigated in our previous work.¹⁸ It was found that the Li⁺—uracil π complex is less stable than the ground-state geometry (O4 binding) by 138 kJ/mol. Because the halo-substituents are electron withdrawing, halo-substitution should decrease the π electron density and make the π complexes even less favorable. Therefore, calculations of the π complexes of the halouracils were not pursued.

Proton Affinities. The preferred site of protonation to U is also at the O4 position but results in greater structural perturbations. The C=O—H⁺ bond angle is 112.4° with the proton again directed away from the adjacent NH group. This indicates sp² hybridization, in contrast to the C=O—M⁺ bond angles which are nearly linear. Three alternate and less stable proton binding sites are found with similar C=O—H⁺ bond angles (Table 2). The second most favorable binding site is also at the O4 position with the proton directed toward the adjacent NH group. Proton binding at this site is less favorable by 9.7 kJ/mol. The other two favorable binding sites are at the O2 position with the proton directed toward N1H being more favorable than toward N3H. Proton binding at these sites is less favorable than in the ground-state O4 binding conformation by 29.9 and 34.7 kJ/mol, respectively. The results for proton binding to the XU nucleobases are very similar to that found for U. In all cases, halogenation decreases the proton affinity (PA) of all four binding sites by 2.0 to 30.9 kJ/mol. The decrease in PA is the smallest for 5-IU and increases as the size of the halogen atom decreases. The O4 sites are destabilized to a greater extent than the O2 sites in the 5-XU systems, whereas the reverse is true for 6-ClU. These differences in the stabilization of the O2 and O4 sites result in different relative PA orderings for binding at these sites.

Acidities. Although uracil is one of the five nucleobases, it exhibits acidic character as well. Biologically, the two NH bonds in uracil affect its hydrogen bonding capabilities as well as the activities of enzymes for which uracil is a substrate. The calculated gas-phase acidities of uracil and its halogenated analogues are summarized in Table 5. Also listed in Table 5 are literature values for the measured and calculated acidities of uracil.^{53,54,55} Our calculations find that the N1 position of uracil is considerably more acidic than the N3 position, by 49.4

kJ/mol. In previous work, we also calculated the acidities of uracil at the CBS-Q level of theory.¹⁸ Those calculations suggested that MP2 overestimates the N1 and N3 acidities of U but showed that the relative acidities were accurately reproduced. Thus the trends in the MP2 acidities should be a good descriptor of the influence of halogenation on the acidity of the N1 and N3 sites. The measured acidities also confirm that the N1 site is more acidic than the N3 site, but by a greater difference than suggested by theory, 59 kJ/mol. Halo-substitution leads to an increase in the acidity of both sites. The acidity of the N3 site is relatively insensitive to the position and identity of the halogen atom and increases by 26.6 to 31.6 kJ/mol across these systems. In contrast, the acidity of the N1 site is sensitive to both the position and identity of the halogen atom. In the 5-XU systems, the N1 site becomes more acidic as the size of the halogen atom increases, by 18.7 to 30.3 kJ/mol. Comparison of the 5-ClU and 6-ClU systems indicates that 6-halo-substitution produces a much larger increase in the acidity of the N3 site, 18.7 versus 43.9 kJ/mol, respectively.

Base Pairing. In nucleic acids, uracil and thymine base pair with adenine via two hydrogen bonds in which the O4 and N3H atoms of U (T = 5-MeU) interact with one of the amino H atoms and N1 of adenine (A), respectively. In the calculations performed here, we only consider such Watson—Crick base pairing. The base pairing energy of the A::U base pair is calculated to be 51.0 kJ/mol. Halogenation is found to increase the pairing energy by 1.4 to 2.6 kJ/mol. In all cases, the base pairs are planar. The structures of these bases pairs are shown in Figure 5 and are listed in Table 3S of the Supporting Information. Modest variations in the (NH···N and NH···O) hydrogen bond lengths are observed, Table 6. The NH···N hydrogen bond length decreases by 0.018–0.105 Å, with the largest decreases observed for the A::5-FU and A::5-ClU systems. This is somewhat compensated for by a large increase in the NH···O hydrogen bond length for the A::5-FU and A::5-ClU systems, 0.056 Å. In contrast, the NH···O hydrogen bond length increases by a much smaller amount in the other base pairs, 0.012–0.022 Å.

Discussion

Comparison between Theory and Experiment. The alkali metal ion affinities of the XU nucleobases at 0 K measured by guided ion beam mass spectrometry and calculated here are summarized in Tables 2 and 3. The agreement between theory and experiment is illustrated in Figure 6. It can be seen that the agreement is quite good for the Na⁺(XU) and K⁺(XU) complexes, but less satisfactory for the Li⁺(XU) complexes. The mean absolute deviation (MAD) between experiment and theory for all 14 systems is 14.1 ± 15.2 kJ/mol. This is somewhat larger than the MAD between theory and experiment found for a variety of Na⁺ complexes calculated at this level of theory (~8 kJ/mol).¹⁸ This is also larger than the average experimental error of 5.1 ± 1.9 kJ/mol. However, it is clear that principal contributors to the deviations are the Li⁺(XU) systems. For the four Li⁺(XU) systems, the MAD is 33.3 ± 16.1 kJ/mol, whereas the MADs for the Na⁺(XU) and K⁺(XU) systems are much smaller, 8.2 ± 4.7 kJ/mol and 4.7 ± 3.8 kJ/mol, respectively. Theory systematically underestimates the BDEs for the Li⁺(XU) complexes. This disparity may be a result of the higher degree of covalency in the Li⁺—nucleobase interaction. The additional covalency of the alkali metal ion—

(53) Kurinovich, M. A.; Lee, J. K. *J. Am. Chem. Soc.* **2000**, *122*, 6258.

(54) Nguyen, M. T.; Chandra, A. K.; Zeegers-Huyskens, T. *J. Chem. Soc., Faraday Trans.* **1998**, *94*, 1277.

(55) Kurinovich, M. A.; Lee, J. K. *J. Am. Soc. Mass Spectrom.* **2002**, *13*, 985.

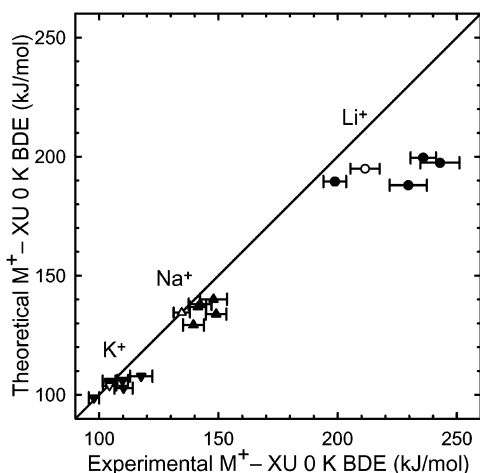


Figure 6. Theoretical versus experimental 0 K bond dissociation energies of $M^+–XU$ (in kJ/mol, where $M^+ = Li^+$ (●, ○), Na^+ (▲, △), and K^+ (■, □) and $XU = U, 5-FU, 5-CIU, 6-CIU, 5-BrU,$ and $5-IU$). Values for uracil are shown as open symbols.¹⁸

nucleobase interaction in the Li^+ systems compared to those for Na^+ and K^+ suggests that this level of theory may be inadequate for a complete description of the former systems. In previous studies where similar results were found for binding of various ligands (including uracil) to Li^+ , Na^+ , and K^+ , we performed additional calculations using the complete basis set extrapolation protocol, CBS-Q, and compared the measured BDEs to those calculated at this level of theory. In all cases, the agreement between theory and experiment improved for the Li^+ systems.^{19,56} Attempts were made in the present work to perform calculations using the CBS-Q complete basis set extrapolation protocol for the $M^+(XU)$ complexes, but unfortunately the presence of the halogen substituent put these calculations beyond the computational resources available to us. Because such disparities have been observed for other Li^+ –(ligand) complexes previously investigated in our laboratory, this issue will be the subject of future work.

Influence of Using ECPs on the Computation Results. As discussed above, parameters for iodine are not available in the 6-31G* and 6-311+G(2d,2p) basis sets employed in this work, necessitating the use of ECPs to describe the iodine atom. To assess the accuracy of these results, we performed calculations for the $M^+(5-BrU)$ systems using the above basis sets as well as ECPs to describe the Br atom. According to Check et al.,⁴² the use of additional polarization and diffuse exponents for the LANL2DZ basis set for elements in groups 14–17 substantially improves the accuracy of calculated electron affinities, vibrational frequencies, bond lengths, and BDEs. Therefore, we employed both the LANL2DZ and modified LANL2DZ basis sets for the Br and I atoms.^{40–42} The computed $M^+(XU)$ BDEs are listed in Tables 2 and 3. Comparison of the $M^+(5-BrU)$ BDEs calculated at these three levels of theory shows that the ECPs do a very good job of describing these systems. Slightly better agreement between the ab initio and modified LANL2DZ is found compared to the standard LANL2DZ ECPs. Similar results were found by Check et al. in which the modified basis set leads to improved energetics computation for determination of X_2 and X_3^- cluster BDEs, where $X = F, Cl,$ and Br .⁴² The

computational results based on the modified LANL2DZ basis set are expected to be slightly more reliable and were therefore used for comparison to the experiment values.

Another interesting observation is the influence of the standard and modified basis set on the calculated BDEs. The calculated PAs decrease by 1.5 to 5.7 kJ/mol when the basis set is expanded from LANL2DZ to the modified LANL2DZ, regardless of the binding position. In contrast, the $M^+(XU)$ BDEs increase by 1.2 to 3.8 kJ/mol for binding at O4, while they decrease by 2.5 to 3.4 kJ/mol for binding at O2.

Conversion from 0 to 298 K. The 0 K BDEs determined here are converted to 298 K bond enthalpies and free energies. The enthalpy and entropy conversions are calculated using standard formulas and the vibrational and rotational constants determined for the MP2(full)/6-31G* optimized geometries, which are given in Tables 1S and 2S. Table 4S lists 0 and 298 K enthalpy, free energy, and enthalpic and entropic corrections for all $M^+(XU)$ systems experimentally determined along with the corresponding theoretical values (Tables 2 and 3).

Trends in the Binding of Alkali Metal Ions to the Halogenated Uracils. In all of the $M^+(XU)$ systems, the measured BDE varies with the alkali metal ion such that Li^+ binds ~60% more strongly than Na^+ , which in turn binds ~35% more strongly than K^+ . Because these complexes are largely electrostatic in nature, this is easily understood based upon the size of the metal ion. The smaller the ion, the shorter the metal–ligand distance, and therefore, the greater the strength of the ion–dipole and ion-induced dipole interactions.

Theoretical examination of the Mulliken charges retained by the alkali metal ion in these complexes shows that, for the $M^+(XU)$ complexes, Li^+ retains less charge (0.49–0.83 e) than Na^+ (0.81–0.88 e), which retains less charge than K^+ (0.92–0.97 e). These results confirm the electrostatic nature of the bonding but also demonstrate that there is some covalency in the alkali metal ion–nucleobase interaction, especially in the $Li^+(XU)$ systems. In these systems, the shorter $Li^+–O$ bond distance allows the alkali metal ion to more effectively withdraw electron density from the neutral XU nucleobase thus reducing the charge retained by the alkali metal ion.

Influence of Halogenation of the Alkali Metal Ion Binding Affinities of Uracil. As discussed above, the variation in the $M^+–XU$ BDEs with alkali metal ion indicates that the binding in these complexes is largely electrostatic. Therefore, the strength of the binding in these complexes should be controlled by ion–dipole and ion-induced dipole interactions. The effect that the halogen substituent has upon the binding can be examined by comparing these $M^+(XU)$ systems to the corresponding $M^+(U)$ systems. The strength of the ion–dipole interactions should correlate with the magnitude of the dipole moments of U and the XU nucleobases and the alignment of the alkali metal ion with the dipole moment vector in the $M^+(U)$ and $M^+(XU)$ complexes. As discussed above, 5-halogenation results in an ~10% decrease in the dipole moment, whereas 6-halogenation leads to a greater decrease of ~25%. This would suggest that the binding in all of the $M^+(XU)$ complexes should be weaker than that in the $M^+(U)$ complexes. However, this conclusion ignores the alignment of the alkali metal ion with the dipole moment of the nucleobase, which improves in the order $6-CIU < 5-FU < U < 5-CIU < 5-BrU < 5-IU$ for the ground-state complexes (O4 binding) suggesting

(56) Rannulu, N. S.; Amunugama, R.; Yang, Z.; Rodgers, M. T. *J. Phys. Chem. A* **2004**, *108*, 6385.

the $M^+(U)$ and $M^+(XU)$ BDEs should follow this same order if the ion–dipole interactions dominate the binding. Examination of the theoretical data shows that this order is preserved for all three alkali metal ions. However, the trends in the experimental data are not as consistent but generally follow this same trend. The strength of the ion-induced dipole interactions should correlate with the polarizability of the neutral nucleobase. The polarizability is not expected to vary significantly with the position of halogenation, and the additivity method we used to estimate these polarizabilities is not sensitive to such structural differences. As summarized in Figure 1, the polarizability of these nucleobases follow the order: $U \approx 5-FU < 5-CIU \approx 6-CIU < 5-BrU < 5-IU$. This suggests that if the ion-induced dipole interactions dominate the binding, the $M^+(U)$ and $M^+(XU)$ BDEs should follow this same order. Clearly this is not the case, suggesting that the ion–dipole interactions dominate, while the ion-induced dipole interactions exhibit a lesser effect on the strength of the binding in these systems.

Further examination of the Mulliken charge retained by the alkali metal ion in these complexes shows that it decreases with increasing size of the halogen substituent in the $M^+(5-XU)$ complexes. This trend makes sense because the interaction between the alkali metal ion and the halogen atom should become more covalent as the electronegativity of the substituent decreases. In addition, the $M^+(5-XU)$ complexes retain less charge than the $M^+(6-CIU)$ complexes. Again this trend makes sense because the halogen substituent does not contribute to the binding in the latter complexes, whereas the halogen substituent is able to donate electron density to the alkali metal ion in the former complexes thus reducing the charge on the alkali metal ion.

Influence of Halogenation on the Proton Affinity of Uracil.

The calculated proton affinities (PAs) of U and the XU nucleobases are summarized in Tables 2 and 3. Also given in Table 2 is the measured proton affinity of U determined from ion–molecule reaction bracketing studies.^{57,58} In all cases, halogenation results in a decrease in the PA of uracil. The reduction in the PA is largest for the most electronegative halogen substituent, F, and decreases with increasing size (or decreasing electronegativity) of the halogen substituent for the 5-XU systems. Thus the trend in the PAs of the 5-XU nucleobases parallels that for the $M^+(5-XU)$ BDEs. The PA of 6-CIU does not follow this simple trend, falling between the values for 5-BrU and 5-IU, whereas the $M^+(6-XU)$ BDEs are smaller than those for the corresponding $M^+(5-XU)$ complexes. The very small size of the proton does not allow it to chelate with the halogen substituent in the $H^+(5-XU)$ systems. Thus, the identity of halogen substituent exerts only a small influence on the PA. This contrasts the behavior seen in the $M^+(5-XU)$ complexes, where the larger size of the alkali metal ion allows such chelation to occur producing a more significant effect on the BDEs.

Influence of Halogenation on the Acidity of Uracil. The calculated acidities of U and the XU nucleobases are summarized in Table 5. Also given in Table 5 are literature values

for the acidity of U calculated at the CBS-Q,¹⁸ B3LYP/6-31++G**,⁵⁴ and B3LYP/6-31+G**⁵⁵ levels of theory and values measured by ion–molecule reaction bracketing studies.⁵³ In all cases, halogenation results in an increase of the acidity of uracil that is strongly dependent upon the position of halogenation, but only moderately influenced by the identity of the halogen, substituent (i.e., the acidity increases by 18.7 to 30.3 kJ/mol for the 5-XU nucleobases and by 43.9 kJ/mol for 6-CIU). Among the 5-XU nucleobases, the increase in the acidity is smallest for the most electronegative halogen substituent, F, and increases with increasing size of the halogen substituent. Thus the influence of halogenation on the acidities of the 5-XU nucleobases parallels that for the binding of alkali metal ions to these nucleobases.

Implications for Nucleic Acid Stability. The present results allow predictions for metal-induced and halogenation-induced stability changes in nucleic acids. In previous work we examined the metal-induced stability changes by examining the influence of binding Na^+ to the A::U base pair.¹⁸ Binding of Na^+ to the O2 and O4 sites of the A::U base pair was found to be more than 28.3 and 45.5 kJ/mol more favorable than binding to the N7/NH2 and N3 sites of A. In addition, binding of Na^+ to A::U was found to increase the pairing energy by 17.0 to 48.9 kJ/mol and therefore suggests that alkali metal cationization should increase the stability of nucleic acids. However, alkali metal cationization causes the A::U base pair to distort from planarity and could weaken hydrogen-bonding interactions between nearby base pairs. This would reduce the stabilization gained from the additional chelation interactions with the alkali metal ion and impact the stability of the nucleic acid to a lesser extent than for the isolated base pair. The presence of the alkali metal ion would also tend to increase the strength of base stacking interactions via cation– π interaction of the alkali metal ion with the adjacent nucleobases. These effects can be expected to be somewhat larger for the XU nucleobases than those found for U because the halogen substituent increases the binding affinity of alkali metal ions. Thus, alkali metal ion binding to the XU nucleobases should increase the stability of nucleic acids by reducing the charge on the nucleic acid via a zwitterion effect as well as through additional noncovalent interactions between the alkali metal ion and the nucleobases.

Previous work has shown that 5-fluoro substitution of uracil increases the acidity of N3H and alters the dynamical properties and thermal stability of nucleic acids.^{1,6,59} In addition, experiments have provided evidence that 5-FU incorporation into DNA and RNA produces changes in the secondary structure, thermal stability, and can result in miscoding during protein synthesis.^{6,60,61,62} The present results confirm that the N3H position becomes more acidic upon halogenation of uracil. Indeed, halogenation alters many properties of uracil, e.g., dipole moment, polarizability, acidity, basicity, and its interactions with alkali metal ions. As discussed above, in double stranded DNA, thymine base pairs with adenine via two hydrogen bonds in which the O4 and N3H atoms of T interact with one of the amino H atoms and N1 of A, respectively. The enhanced acidity

(57) Hunter, E. P.; Lias, S. G. Proton Affinity Evaluation. In *NIST Chemistry WebBook, NIST Standard Reference Database Number 69*; Mallard, W. G.; Lindstrom, P. J., Eds.; National Institute of Standards and Technology: Gaithersburg, MD, November, 1998; 20899 (<http://webbook.nist.gov>).

(58) Kurinovich, M. A.; Phillips, L. M.; Sharma, S.; Lee, J. K. *Chem. Commun.* **2002**, 2354.

(59) Danenberg, P. V.; Shea, L. C. C.; Danenberg, K. *Cancer Res.* **1990**, *50*, 1757.

(60) Dolnic, B. J.; Pink, J. J. *J. Biol. Chem.* **1985**, *260*, 3006.

(61) Armstrong, R. D.; Takimoto, C. H.; Cadman, E. C. *J. Biol. Chem.* **1986**, *261*, 21.

(62) Sowers, L. C.; Eritja, R.; Kaplan, B. E.; Goodman, M. F.; Fazakerley, G. V. *J. Biol. Chem.* **1987**, *262*, 15436.

of the N1H position would tend to decrease the stability of halogenated nucleic acids, making the base more susceptible to cleavage of the glycosidic bond. The N1 hydrogen is also lost during RNA formation, and therefore the enhanced N1H acidity might also affect the dynamics of DNA transcription. During the transcription of DNA, U and A comprise the base pairs. It is known that the stability of DNA is controlled by the strength of hydrogen bonding in the base pairs as well as stacking interactions between adjacent base pairs. The strength of hydrogen bonding in the A::U (A::T) base pairs is controlled by the acidity of N3H and the PA of the less favorable O4 binding site. The decrease in the PA of this site upon halogenation would tend to weaken the hydrogen bonding interactions in the A::XU base pairs. In contrast, the greater acidity of the N3H position would tend to make this site a better proton donor, resulting in stronger hydrogen bonding interactions. Overall these effects nearly cancel and lead to a small increase in the stability of the A::XU base pairs. Theoretical studies^{63,64} have shown that, in DNA, the stacking interaction between the nucleobases is mainly controlled by dispersion energy, which is proportional to the polarizabilities of the interacting molecules. These studies^{63,64} also concluded that the nucleobases stack in the antiparallel direction of the dipole moments as the result of dipole–dipole interactions between nucleobase pairs. Because halogenation alters the magnitude and direction of the dipole moment as well as the polarizability of U, these changes might induce minor conformational changes in DNA and alter the strength of the stacking interactions, both of which are likely to produce additional effects upon their functions as suggested by previous studies. These effects are expected to be somewhat smaller for 5-halogenated uracils than 6-halogenated uracils because the changes in the magnitude and direction of the dipole moment are less significant in the former species.

Conclusions

The kinetic energy dependence of the CID of $M^+(XU)$, where $M^+ = Li^+, Na^+, \text{ and } K^+$ and $XU = 5-FU, 5-CIU, 6-CIU, 5-BrU,$ and $5-IU$, with Xe is examined in a guided ion beam mass spectrometer. The dominant dissociation process is loss of the

intact neutral XU nucleobase. Thresholds for these processes are determined after consideration of the effects of reactant internal energy, multiple collisions with Xe, and lifetime effects. Insight into the structures and binding of alkali metal ions to the XU nucleobases as well as the effects of halogenation on the proton affinities, acidities, and base pairing energies is provided by ab initio calculations. Very good agreement between the experimentally determined and theoretically calculated alkali metal ion affinities is obtained for the $Na^+(XU)$ and $K^+(XU)$ complexes, suggesting that these ligands can act as reliable anchors for the alkali metal ion affinity scales and broaden the range of ligands available as absolute thermochemical anchors. The calculated BDEs for the $Li^+(XU)$ complexes are found to be systematically lower than the values measured here. These discrepancies are not completely understood but appear to be a result of several subtle electronic effects that may require higher levels of correlation to accurately predict the BDEs in the $Li^+(XU)$ systems. Further, the combined experimental and theoretical results provide an understanding of the influence of alkali metal ion binding and halogenation on the structure and stability of nucleic acids. Alkali metal ion binding is expected to increase the stability of nucleic acids by reducing the charge on the nucleic acid in a zwitterion effect as well as through additional noncovalent interactions between the alkali metal ion and the nucleobases. Halogenation is found to further influence the stability of nucleic acids by decreasing the proton affinity of uracil and increasing the alkali metal ion binding affinity and acidity of uracil, as well as the stability of A::U base pair.

Acknowledgment. This work is supported by the National Science Foundation, Grant CHE-0138504.

Supporting Information Available: Tables of vibrational frequencies, average vibrational energies at 298 K, and rotational constants. MP2(full)/6-31G* geometry optimized structures, geometrical parameters, and enthalpies and free energies of M^+ binding to XU. Figures showing cross sections for the collision-induced dissociation of $M^+(XU)$ with Xe as well as empirical fits to the primary product channels, $M^+ = Li^+, Na^+, \text{ and } K^+$ and $XU = 5-FU, 5-CIU, 6-CIU, 5-BrU,$ and $5-IU$. This material is available free of charge via the Internet at <http://pubs.acs.org>.

JA045375P

(63) Hóřba, P.; Šponer, J.; Poláček, M. *J. Am. Chem. Soc.* **1995**, *117*, 792.
(64) Šponer, J.; Leszczyński, J.; Hóřba, P. *J. Phys. Chem.* **1996**, *100*, 5590.